STRENGTH OF MULTI-BOLT HYBRID BONDED/BOLTED COMPOSITE JOINTS: A PARAMETRIC STUDY ON GEOMETRIC PARAMETERS

Valentin S. Romanov*, Jung Bae and Larry Lessard

Department of Mechanical Engineering, McGill University, Montreal, Canada

* Corresponding author (valentin.romanov@mcgill.ca)

Keywords: Multi-bolt joints, Hybrid bolted/bonded joints, Kinematic model, Mechanical properties

ABSTRACT

The present experimental work executes a parametric study on single-lap hybrid bonded/bolted composite joints with multiple bolts. Joints of five different geometric configurations are subjected to the static tensile tension. The results indicate a significant influence of the overlap length on the strength values, whereas, although considerable, the impact of the edge distance is not proven to be consistent. Joint stiffness is shown to be mainly governed by the overlap length. The load sharing between the adhesive and the bolts is proven to be geometry-dependent: facilitated by a shorter joint overlap length and smaller edge distance. Better bolt load sharing, however, does not result in higher strength. The experimental results are in a good agreement with the modeling obtained using the Hybrid Joint Engineering Tool proving that the latter can be effectively used for the strength prediction of complex multi-bolt scenarios in hybrid bolted/bonded joints.

1. INTRODUCTION

The joining of composite materials has traditionally been achieved by mechanical fastening or adhesive bonding. Recent studies on a combination of these two techniques – hybrid bonded/bolted joining – showed a potential for a higher strength as compared to the bonded and bolted joints separately [1, 2]. This was shown to be achievable only by a particular combination of materials and geometrical parameters [3-5]. First, the adhesive has to be flexible and of a viscoelastic nature to facilitate the load transfer to the bolts without failure. Other key aspects for the strength of the hybrid joint are the adhesive thickness, the bolt positioning and the overlap area of the joint.

While some studies exist on the bolted joints with multiple bolts and on the effect of the respective geometric parameters on the joint strength [6], the effect of the latter in multi-bolt hybrid joints is not well-understood. The present experimental work executes a parametric study on single-lap hybrid bonded/bolted composite joints with multiple bolts. The focus of this qualitative study is put on the influence of geometric parameters – such as the edge distance to the bolts and the distance between the bolts – on the joint static behavior and its mechanical properties such as strength. The experimental study is to be supported with the modeling results obtained with an in-house design tool developed at McGill University.

2. MATERIALS AND METHODS

2.1 Materials

The composite, bolt and adhesive materials are kept constant throughout the study. The composite substrates are the quasi-isotopic carbon/epoxy laminates made of Cycom 5320 carbon fiber prepreg, whose properties are provided in Table 1. The substrate layup is $[45/0/-45/90]_{4s}$.

E_{11} (GPa)	$E_{22}=E_{33}$ (GPa)	$G_{12}=G_{13}$ (GPa)	G_{23} (GPa)	ν_{23}
141	9.7	5.1	3.4	0.34

Table 1. Cytec 5320 CFRP tape properties

To facilitate the load sharing, a ductile and low-yielding epoxy adhesive is chosen to bond the substrates. A two-part Hysol EA-9361 adhesive, with an elastic modulus of E_a = 559 MPa, Poisson's ratio of ν_a = 0,42, yield strength of σ_y = 9 MPa and strain hardening of H = 34,5 MPa is used. The steel bolt properties are E_b = 205 GPa, ν= 0,3.

2.2 Joint design and manufacturing

The substrates and doublers were manufactured using the following procedure:

1. A flat plate was laid up with the prepreg sheets using a stacking sequence according to the chosen layup. A vacuum cure was performed using the manufacturer recommended cure cycle.
2. The plate was cut with a diamond-tipped saw to obtain the substrates and doublers.
3. For a precise control of the substrate alignment, the components were assembled and bonded inside a custom-built jig [7]. The joint overlap length, bondline thickness and spew filet geometry was controlled by the aluminum spacers.
4. To ensure uniform mixing and de-aeration, the two parts of Hysol EA-9361 adhesive were mixed using a Thinky ARE-310 centrifugal mixer. After that the adhesive was cured in an oven.
5. Using a computer numerical control drill, bolt holes were drilled in the joint overlap according to the geometry set-ups described in the next section. No delamination or fiber pullout damage was visually evident following the drilling. The diametric tolerance of holes was within 8 mm +25.4/-0 µm.
6. Misumi GDMSB8-13-F10-M8 steel bolts were installed with DIN-125 flat washers on either side of the joint between the bolthead and metric M8 heavy hex nut. The latter was finger tightened.

2.3 Parametric study

Each joint is represented by composite substrates bonded with a flexible epoxy adhesive and fastened by two steel bolts along the centerline of the joint. Figure 1(a) provides schematics of a typical joint set-up. The parameters that define the joint geometry are the substrate length L, substrate width W, substrate thickness t, adhesive thickness t_a, overlap length La, edge distance to the bolts E, hole diameter D, bolt head diameter D_h and distance between the bolts L_j.

Five different geometry configurations are considered, varying E, L_j and L_a to capture the influence of these parameters on the joint static behavior. The configuration parameters are gathered in Table 2, while Figure 1(b) gives an overview of the geometric cases.

2.4 Kinematic model

The experimental results are to be compared to those of modeling, obtained with the Hybrid Joint Engineering Tool (HJET) [8] developed by Romanov at McGill University. This design tool employs the kinematic model developed by Bodjona and Lessard [9] based on a modified shear lag theory. The model is presented for the static stress analysis of a composite bonded/bolted single-lap joint. Its formulation takes into account the nonlinear adhesive constitutive behavior, bolt-hole clearance, bolt clamp-up and contact. The model was previously validated by comparison with finite element analysis and experimentally. For a detailed description of the model, the reader is referred to the original paper [9].

2.5 Failure criteria

Among different failure criteria that HJET accommodates, the point stress Yamada-Sun failure criterion [10, 11] for the substrates and the maximum strain criterion for the adhesive are chosen for the present study.

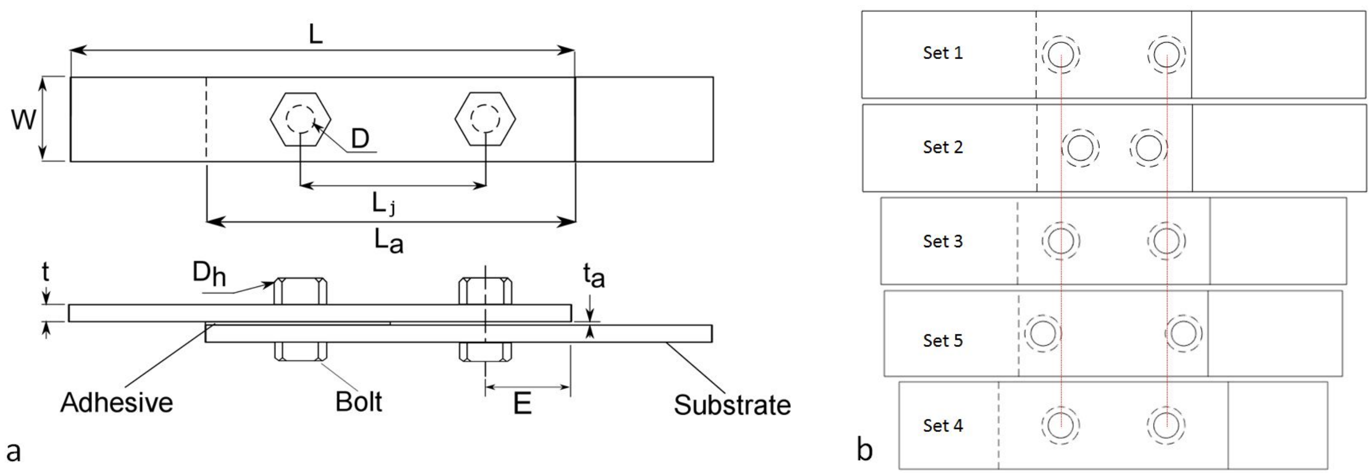

Figure 1. Multi-bolt hybrid joint: (a) schematics; (b) geometry configurations indicating relative difference in positioning of bolts and overlap.

	Set 1	*Set 2*	*Set 3*	*Set 4*	*Set 5*
Overlap length (*La*)	50	50	62	74	62
Edge distance (*E*)	8	14	14	20	8
Bolt distance (L_j)	34	22	34	34	46
Width (*W*)			28		
Adhesive thickness (t_a)			0.3		

Table 2. Parametric study: joint geometry [mm].

2.6 Test procedure

The focus of this qualitative study is put on the influence of these geometric parameters on the joint static behavior and its mechanical properties such as stiffness and strength. All joints are subjected to the static tensile tension using a 100 kN hydraulic MTS tensile testing machine. The applied load is adjusted to remove any tensile/compressive load imparted on the specimen due to clamping. The load and crosshead displacement are recorded during testing. All tests are performed under room temperature and dry conditions. To minimize the effect of other external influences, the tests for all joint configurations are performed in the same day.

The digital image correlation (DIC) technique is used for capturing the joint strain maps developed throughout testing. For this, the specimens were covered with the white paint followed by laying the speckle pattern with a black paint spray. This can be noticed in specimen images shown in Figure 3. However, due to lack of space, the results obtained via DIC are not covered in the present manuscript but will be reported in a future peer-reviewed journal publication.

3. RESULTS AND DISCUSSION

The experimental load/displacement envelopes of all sets are shown in Figure 2(a). The sample experimental results are accompanied with the analysis results presented in Figure 2(b) for comparison. The experimental and model curves are not directly compared on the same plot since the experimental displacement is that of the crosshead recorded throughout the tests. This includes machine displacement, grip displacement, etc., and is, therefore, not directly comparable with the joint displacement calculated by the model which does not take into account these testing features. Thus, only qualitative stiffness comparison is present. Some of the specimens were subject to internal defects which effect become more significant as the applied load rises. This resulted in the load/displacement envelope openings close to the failure loads in some of the sets.

Comparing the curves, the measured stiffness can be put in the following descending order: that of Set 4 with the largest overlap length (74 mm), then of Set 3 and Set 5 (62 mm), and then of Set 1 and Set 2 (50 mm). This confirms the hypothesis that joint stiffness is governed by the adhesive area. Bolt positioning, on the other hand, – hence, edge distance – does not affect joint stiffness. The model curves capture this exact tendency standing out clearly in the three sets of joint stiffness, indicating similar behavior of joints with the same overlap length.

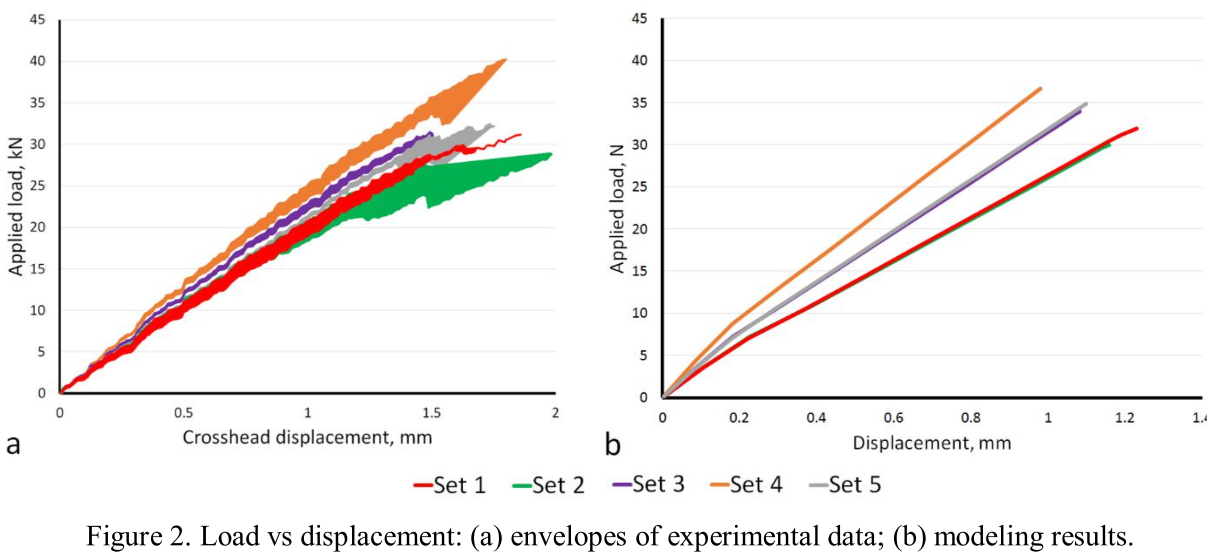

Figure 2. Load vs displacement: (a) envelopes of experimental data; (b) modeling results.

Failure modes observed during testing can be found in Figure 3. In the present experimental study, joint failure was not consistent in terms of instantaneity. In all the sets, prior to failure all samples produced loud cracking, indicating damage and/or delamination within substrates. Only approximately one half of the specimens failed abruptly with no separation between the damage stages. Some specimens, on the other hand, showed more complex damage evolution. In these, the adhesive damage occurred the first leaving the fastened substrates to carry all the applied load. Only then this was followed by delamination and an ultimate failure of one of the substrates. In addition, the adhesive damage was also not consistent: as well as partial, the full bondline adhesive failure occurred in all the sets seemingly being not affected by the overlap length.

Most samples in all sets failed with the net-section failure mode (Figure 3(c)). Yet, several specimens, primarily in sets 1 and 5, failed with the shear-out failure mode. This is attributed to the small $E/D = 1$ ratio in these sets.

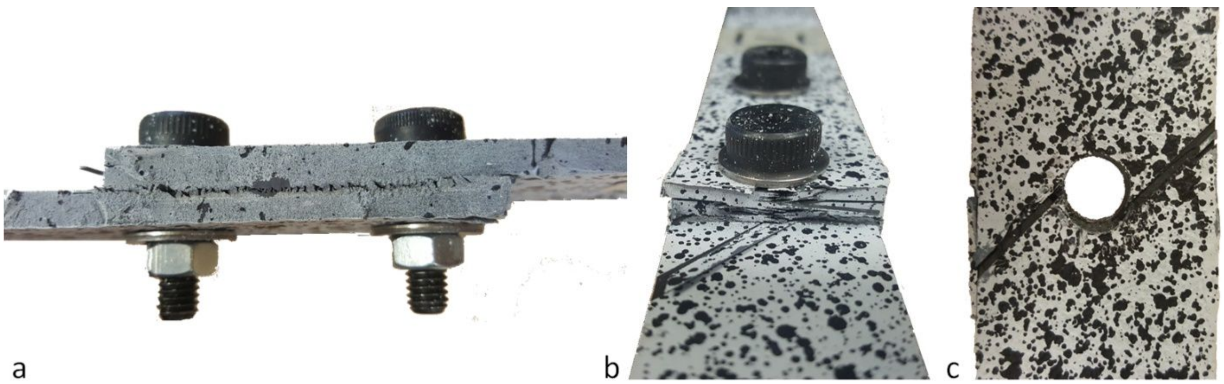

Figure 3. The observed failure modes: (a) adhesive bondline failure; (b) shear-out substrate failure; (c) net-section substrate failure.

The strength values obtained experimentally are plotted together with the modeling predictions in Figure 4. The experimental values are the average of data from four samples within each set. The predicted values correlate with the experimental data well, and in most cases the error was within 10%. The results indicate that joint strength is mainly controlled by adhesive area with a minor effect of bolt distance to the overlap edge. In addition to higher stiffness, longer joint overlap also results in higher loads that the hybrid joint can sustain.

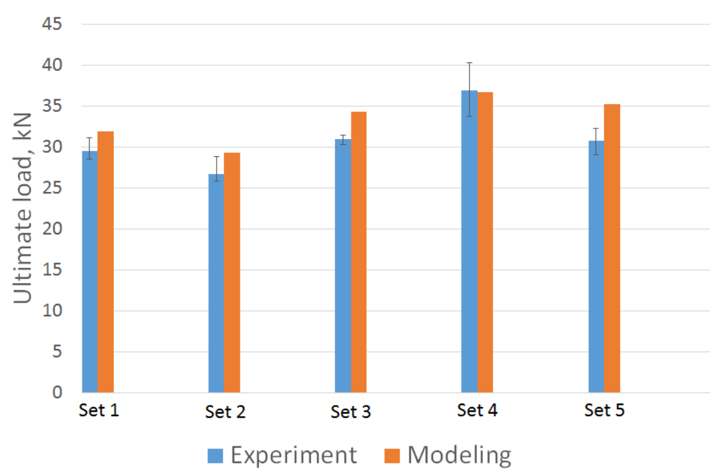

Figure 4. Joint strength values.

Interestingly, this contradicts the findings regarding the bolt load sharing. As was reported in literature [3-5], bolt load sharing plays a significant role in hybrid bolted/bonded joint static behavior including joint strength improvement. This, however, is not completely in agreement with the present study. According to the modeling results, better load sharing does not necessarily improve overall joint strength. This can be clearly seen in Figure 5(a), where the load taken by bolts relative to the applied load is plotted versus the total applied load. The curves correspond to three configurations – Sets 1,3,4 – with the same L_j = 34 mm but different L_a – 50, 62 and 74 mm, respectively – put in the ascending order. As L_j stays constant, E is proportional to L_a. It is noted that while the bolt load sharing drops from 40% of total applied load to 32% to 25% as L_a increases in value, the overall joint strength increases from 31.9 kN to 34.3 kN to 36.7 kN. In relative terms, an increase of L_a by 24% and 48% drops the bolt load sharing by 20% and 37.5%, respectively. At the same time, it increases the strength by 7.5% and 15%, respectively.

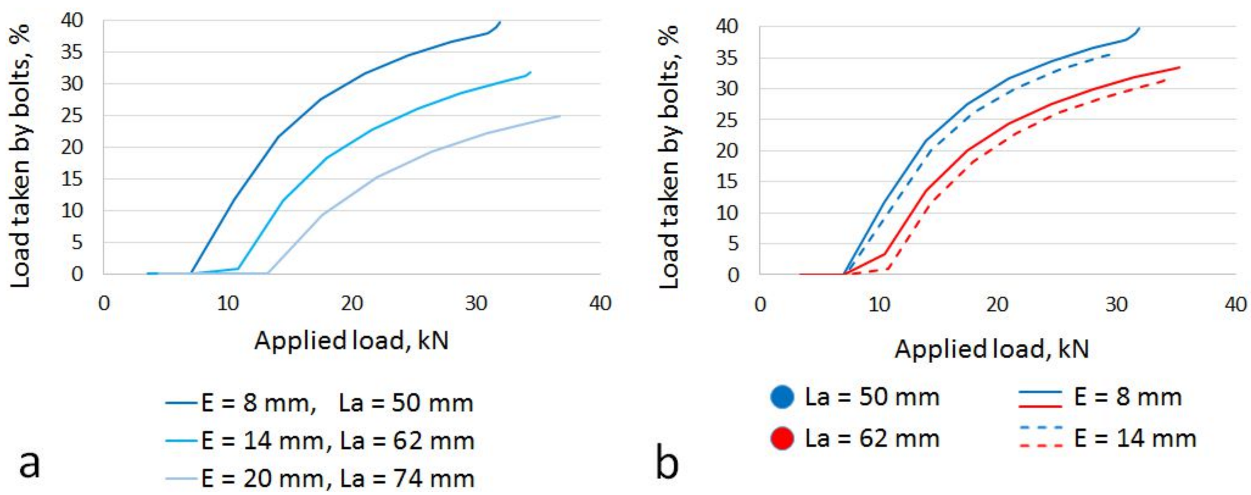

Figure 5. Bolt load sharing.

This tendency can also be seen in Figure 5(b) where comparison among Sets 1,2,3,5 is depicted. The blue color represents joints with L_a = 50 mm, whereas the red color – 62 mm; the solid lines represent joints with E = 8 mm, and the dashed lines – E = 14 mm. Even though the joint strength is proportional to L_a, it drops slightly with a longer E.

The conclusion on the dependency of the overall joint strength to the edge distance and to the bolt load sharing is yet to be drawn. For this, a further investigation is required, supported by a substantial experimental data studying different multi-bolt hybrid joint configurations with a range of different adhesives.

4. CONCLUSIONS

The results indicate a significant influence of the overlap length on the strength values, whereas, although considerable, the influence of the edge distance is not proven to be consistent. The overlap length is also shown to be a major factor governing the hybrid joint stiffness. The hybridization effect of the joint – the load sharing between the adhesive and the bolts – is proven to be geometry-dependent and very sensitive to the presence of adhesive bondline defects.

Bolt load sharing was shown to be facilitated by shorter joint overlap length and smaller edge distance However, better bolt load sharing does not necessarily result in higher strength. Further research is required to provide better understanding of the relation of bolt load sharing in hybrid joints to overall strength.

Finally, the experimental results are compared to those of modeling obtained with the Hybrid Joint Engineering Tool (HJET) developed at McGill University. A good correlation between the modeling and experimental results is observed proving that HJET can be effectively used for the strength prediction of complex multi-bolt scenarios in hybrid bolted/bonded joints.

REFERENCES

[1] M. Fu, P. Mallick, *Fatigue of hybrid (adhesive/bolted) joints in SRIM composites,* International Journal of Adhesion and Adhesives, **21**, 2001, p. 145-59.
[2] N. Chowdhury, W.K. Chiu, J. Wang, P. Chang, *Static and fatigue testing thin riveted, bonded and hybrid carbon fiber double lap joints used in aircraft structures,* Composite Structures, **121**, 2015, p. 315-23.
[3] G. Kelly, *Quasi-static strength and fatigue life of hybrid (Bonded/bolted) composite single-lap joints,* Composite Structures, **72**, 2006, p. 119-29.
[4] C. Bois, H. Wargnier, J.C. Wahl, E. Le Goff, *An analytical model for the strength prediction of hybrid (bolted/bonded) composite joints,* Composite Structures, **97**, 2013, p. 252-60.
[5] G.M. Lehman, A.V. Hawley, D.A.C.L.B. CA., *Investigation of Joints in Advanced Fibrous Composites for Aircraft Structures. Joint and Attachment Investigation. Volume 1. Technical Discussion and Summary*, Defense Technical Information Center, 1969.
[6] C.T. McCarthy, M.A. McCarthy, V.P. Lawlor, *Progressive damage analysis of multi-bolt composite joints with variable bolt–hole clearances,* Composites Part B: Engineering, **36**, 2005, p. 290-305.
[7] K. Bodjona, K. Raju, G.-H. Lim, L. Lessard, *Load sharing in single-lap bonded/bolted composite joints. Part I: Model development and validation,* Composite Structures, **129**, 2015, p. 268-75.
[8] V.S. Romanov, K. Bodjona, L. Lessard, *Design tool for hybrid bonded/bolted composite joints*,
[9] K. Bodjona, L. Lessard, *Nonlinear static analysis of a composite bonded/bolted single-lap joint using the meshfree radial point interpolation method,* Composite Structures, **134**, 2015, p. 1024-35.
[10] F.-K. Chang, R.A. Scott, G.S. Springer, *Failure of Composite Laminates Containing Pin Loaded Holes—Method of Solution,* Journal of Composite Materials, **18**, 1984, p. 255-78.
[11] F.-K. Chang, R.A. Scott, G.S. Springer, *The Effect of Laminate Configuration on Characteristic Lengths and Rail Shear Strength,* Journal of Composite Materials, **18**, 1984, p. 290-6.